

Xiaomian Zhou<sup>1</sup>  
Dayu Liu<sup>1</sup>  
Runtao Zhong<sup>1</sup>  
Zhongpeng Dai<sup>1</sup>  
Dapeng Wu<sup>1</sup>  
Hui Wang<sup>1</sup>  
Yuguang Du<sup>1</sup>  
Zhinan Xia<sup>2</sup>  
Liping Zhang<sup>3</sup>  
Xiaodai Mei<sup>1</sup>  
Bingcheng Lin<sup>1</sup>

<sup>1</sup>Dalian Institute of  
Chemical Physics,  
Chinese Academy of Sciences,  
Dalian, P. R. China

<sup>2</sup>Dana Fabre Cancer Research  
Institute,  
Harvard Medical School,  
Longwood, Boston, MA, USA

<sup>3</sup>Genomic Department,  
Wyeth Pharmaceuticals, Inc.,  
Cambridge, MA, USA

## Determination of SARS-coronavirus by a microfluidic chip system

We have developed a new experimental system based on a microfluidic chip to determine severe acute respiratory syndrome coronavirus (SARS-CoV). The system includes a laser-induced fluorescence microfluidic chip analyzer, a glass microchip for both polymerase chain reaction (PCR) and capillary electrophoresis, a chip thermal cycler based on dual Peltier thermoelectric elements, a reverse transcription-polymerase chain reaction (RT-PCR) SARS diagnostic kit, and a DNA electrophoretic sizing kit. The system allows efficient cDNA amplification of SARS-CoV followed by electrophoretic sizing and detection on the same chip. To enhance the reliability of RT-PCR on SARS-CoV detection, duplex PCR was developed on the microchip. The assay was carried out on a home-made microfluidic chip system. The positive and the negative control were cDNA fragments of SARS-CoV and parainfluenza virus, respectively. The test results showed that 17 positive samples were obtained among 18 samples of nasopharyngeal swabs from clinically diagnosed SARS patients. However, 12 positive results from the same 18 samples were obtained by the conventional RT-PCR with agarose gel electrophoresis detection. The SARS virus species can be analyzed with high positive rate and rapidity on the microfluidic chip system.

**Keywords:** Microfluidic chip system / Miniaturization / Multiplex reverse transcription-polymerase chain reaction / On-line chip polymerase chain reaction / Severe acute respiratory syndrome

DOI 10.1002/elps.200305966

### 1 Introduction

The severe acute respiratory syndrome (SARS), which is an acute respiratory illness caused by a new coronavirus, started to spread around the world in the early spring of 2003 [1]. It is the first major new infectious disease of this century, unusual in its high morbidity and mortality rates. Until now, more than 8000 persons with probable SARS have been diagnosed, 916 patients died. Fortunately, the outbreaks in the initial waves of infection have been brought under control. In the absence of effective drugs or a vaccine for SARS, control of this disease relies on the rapid identification of cases and their appropriate management, including the isolation of suspect and probable cases and the management of their close contacts.

**Correspondence:** Dr. Bingcheng Lin, Dalian Institute of Chemical Physics, Chinese Academy of Sciences, Dalian 116023, P. R. China

**E-mail:** bclin@dicp.ac.cn

**Fax:** +86-0411-84379065

**Abbreviations:** HPMC, hydroxypropylmethylcellulose; RT-PCR, reverse transcription-polymerase chain reaction; SARS-CoV, severe acute respiratory syndrome-associated coronavirus; TBE, Tris-borate-EDTA buffer

Therefore, the establishment of a rapid noninvasive test for this virus is a high priority for detection and control of this disease.

Due to the efforts of the WHO-led international multicenter collaborative network of laboratory testing for SARS, tests for the novel coronavirus have been developed with unprecedented speed [2]. The methods include a molecular test reverse transcription ((RT)-PCR) [3], virus isolation, antibody detection including enzyme-linked immunosorbent assay (ELISA), immunofluorescence assay (IFA), and a neutralization test. But, as SARS epidemic spreads, the specific, rapid, and practical diagnostic tests will become increasingly critical, both for the control of the epidemic and for the management of patients. Among tests, antibody tests detect antibodies produced in response to the SARS coronavirus infection. The determination of different types of antibodies (immunoglobulin M (IgM) and IgG) after SARS-coronavirus (CoV) infection offers a good diagnostic method. However, antibodies apparently increase about 10 days after infection, so the pathogen is undetectable at the early stage of infection. The other effective method is virus isolation in specimens (such as respiratory secretions, blood or stool) from SARS patients, which can be detected by inoculating cell cul-

tures and growing the virus. After isolation, the virus still needs to be identified as SARS virus with further tests. Positive cell culture results indicate the presence of live SARS-CoV in the sample tested and negative cell culture results do not exclude SARS. Cell culture methods are time-consuming and nonspecific. It is unlikely accepted as a universal SARS detection method. The molecular test (RT-PCR) is one of the most commonly used methods for RNA virus detection; it has high sensitivity and can make diagnosis at the early stage [4]. Poon *et al.* [5] reported a real-time quantitative PCR assay, which performed quite well (sensitivity of 79% and specificity of 98%) and it appeared to become positive before antibodies first appeared. It was a good early diagnostic assay for SARS but it was expensive for people in the developing countries. The conventional RT-PCR assay is cheap but the positive rate is lower than the quantitative PCR assays [6]. Therefore, an ideal test for virus will not be only rapid, sensitive, and specific, but also inexpensive and technologically simple, so that it is available at the point of care even in small hospitals or in communities in the developing countries. To achieve the goal, therefore, it is worth studying whether or not the microfluidic chip (lab-on-a-chip) technology can play a role in the early identification of contagion, especially infection of SARS-CoV.

The miniaturization of chemical and mechanical devices for microelectromechanical systems has gained great attention in industry and academic institutions worldwide over recent years. Examples include lab-on-a-chip or microfluidic devices such as on-chip flow-through PCR, microreaction technology, electrophoretic separation devices, *etc.* [7]. These approaches offer novel ways to achieve fast separation with high resolution in a miniaturized fabrication including sample pretreatment steps *i.e.*, sample concentration, labeling, and digestion with the additional possibility of multiplexing. At the same time, there are a lot of alternative methods of DNA analysis on microchips. For example, the TaqMan real-time PCR in silicon-based reactors amplified a variety of DNA and RNA targets [8–10] in order to detect pathogenic viruses and bacteria, plant genes, human genetic diseases, and single nucleotide polymorphism [11, 12]. Although these alternative methods do not provide the DNA sizing information required for a number of biological, biomedical, and forensic analyses, they are useful for various high-throughput applications. The high sensitivity of DNA analysis (detection limit in the order of  $10^{-21}$  mol) [13] had been achieved among those various approaches. Particularly, on-chip PCR provided both rapid, efficient amplification of DNA and low cost [14], and even followed by electrophoretic analysis of the products *in situ* [15]. So, we assume that microfluidic chip

technology may play an important role in the determination of the SARS-CoV of specimens. In this paper, we report a microfluidic chip system to detect this virus in clinical specimens.

## 2 Materials and methods

### 2.1 Chemicals

A 100 mmol/L Tris (Sigma Chemical, St. Louis, MO, USA)/100 mmol/L boric acid/2 mmol/L EDTA buffer (TBE)/2.0% hydroxypropylmethylcellulose (HPMC, 50 cps; Sigma) with a pH of 8.5 was used for separations of 50 ng/ $\mu$ L  $\Phi$ X-174/*Hae*III digest DNA restriction fragments ranging in size from 72 to 1353 bp (TaKaRa Biotechnology, Dalian, China). An approximate 130 ng/ $\mu$ L 100 bp DNA ladder marker ranging in size from 100 to 1500 bp, which is diluted 20-fold in the run buffer, was also purchased from TaKaRa Biotechnology, as well as the PCR products of SARS-CoV. SYTOX Orange nucleic acid stain was obtained from Molecular Probes (Eugene, OR, USA). A 1  $\mu$ mol/L dye solution was prepared in 2.0% HPMC-TBE buffer in order to label DNA on-line. Polyvinylpyrrolidone (PVP) was from Acros (Pittsburgh, PA, USA). A 4.02  $\mu$ M stock solution of Rhodamine 6G dye (Sigma) was prepared in a 100 mM Tris/100 mM boric acid/2 mM EDTA (TBE) buffer, pH 9. Further solutions were prepared by serial dilution of the 4.02  $\mu$ M fluorescein stock solution with the same running buffer for determining the detection limit. All buffers were prepared in doubly distilled water. Solutions were filtered (0.22  $\mu$ m filters) before introduction into the chip.

### 2.2 Samples

The *in vitro* cultured SARS sample was obtained from the autopsied lung tissue of a deceased patient, in whom SARS was diagnosed according to the WHO guidelines [2]. The sample was cultured with Vero-E6 cell line. Total SARS-CoV RNA was isolated from a 210  $\mu$ L cell culture. Eighteen samples of nasopharyngeal swabs of clinically diagnosed SARS patients were from the Nanfang Hospital of the First Military Medical University in Guangzhou. Samples were kept under  $-20^{\circ}\text{C}$  until analysis. The positive control of SARS-CoV is the cDNA fragment of the SARS-CoV sequence, which was provided by BNI (Hamburg, Germany). The negative control of SARS-CoV is the parainfluenza virus. RNA of SARS-CoV was extracted with RNAeasy Mini Kit (Qiagen, Hilden, Germany) before performing the RT-PCR reaction.

## 2.3 RT-PCR

### 2.3.1 RT of RNA

Total RNA from Vero-E6 cell cultures and nasopharyngeal swab samples of clinically diagnosed SARS patients were reversely transcribed to cDNA. Reverse transcription was performed on a GeneAmp PCR system 2400 (Perkin-Elmer, Norwalk, CT, USA) and all reagents used for RT were from TaKaRa Biotech. Two  $\mu\text{L}$  total RNA from cell cultured SARS sample was added to the following RT reaction mixture (20  $\mu\text{L}$ ) containing: 4  $\mu\text{L}$   $\text{Mg}^{2+}$  (25 mmol/L), 2  $\mu\text{L}$  10  $\times$  RNA PCR buffer containing 2.5% PVP, 7.5  $\mu\text{L}$  RNase-free distilled  $\text{H}_2\text{O}$ , 2  $\mu\text{L}$  dNTP mixture (10 mmol/L each), 0.5  $\mu\text{L}$  RNase inhibitor (40 U/ $\mu\text{L}$ ), 1  $\mu\text{L}$  AMV reverse transcriptase XL (5 U/ $\mu\text{L}$ ), and 1  $\mu\text{L}$  Oligo dT-adaptor Primer (2.5 pmol/ $\mu\text{L}$ ). The RT reaction was performed under the following conditions: 10 min at 30°C, 30 min at 50°C, 5 min at 99°C, and 5 min at 4°C.

### 2.3.2 Conventional PCR

The two primer sets of duplex PCR, which were used to determine the cultured SARS-CoV and the samples of the clinically diagnosed SARS patients, were 5'-TAG GATTGCCTACGCAGACT-3' and 5'-AGAGCCATGCCTAACATGCT-3' (for the 240 bp product), and 5'-ATTGGCT GTAACAGCTTGAC-3' and 5'-TAGGGTAACCATTGACTT GG-3' (for the 438 bp product), respectively. The duplex PCR mixture contained 2  $\mu\text{L}$  of the reverse-transcribed product, 5  $\mu\text{L}$  10  $\times$  PCR buffer II, 0.5  $\mu\text{L}$  LA *Taq* DNA polymerase, 1  $\mu\text{L}$  (0.5  $\mu\text{L}$  each of primers) duplex primers (20  $\mu\text{M}$ ), 5  $\mu\text{L}$   $\text{Mg}^{2+}$  (25 mmol/L); sterile water was added to a total volume of 50  $\mu\text{L}$ . The following PCR reaction protocol was employed: 94°C for 5 min followed by 30 cycles at 94°C for 30 s, 55°C for 30 s, 72°C for 30 s, and then 72°C for 7 min. The products of PCR reaction were analyzed by visualizing with ethidium bromide staining. The reaction was finished on the GeneAmp PCR system 2400 (Perkin-Elmer).

## 2.4 Microchip fabrication

The glass microchips were fabricated using standard photolithographic and wet chemical techniques as described elsewhere [16]. The microchannel design in Fig. 1 was transferred onto the substrates using a positive photoresist, photomask, and UV exposure. The microchannels were etched into the substrate in a dilute, stirred

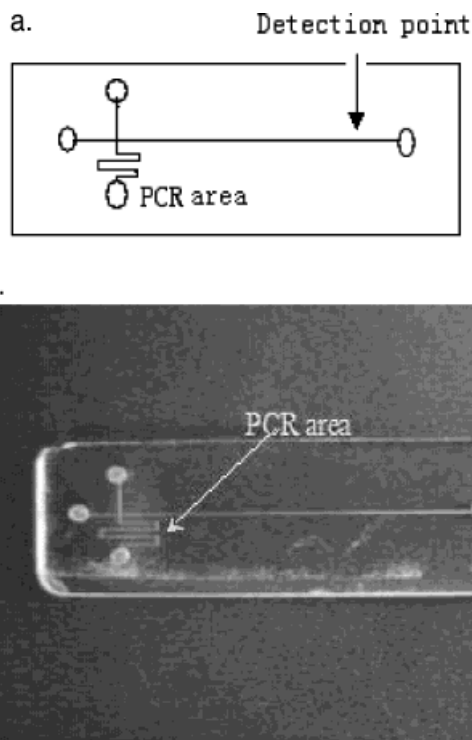


**Figure 1.** (a) Layout of the microfabricated channels; (b) PCR chip. The reactive area includes the reactive pool and the serpent-shape channel. The point of fluorescence detection is marked with an arrow. Potential of sample injection, 400 V/cm at the sample waste; grounding the sample reservoir for 30 s. The buffer and waste reservoirs had no potentials applied. Potentials of separation, 0, 1.1, 0.3, and 0.3 kV at the buffer, waste, sample, and sample waste reservoirs, respectively.

HF/ $\text{NH}_4\text{F}$  bath. To form the closed network of channels, a cover plate was bonded to the substrate over the etched channels by hydrolyzing the surfaces, bringing them into contact with each other, then processing thermally to 200°C in the vacuum oven for 1 h. Subsequently, the pair glass plates were placed between two pieces of smooth China plates and annealed in a Model SX3-4-10 programmable furnace (Zhonghuan Test Electrical Furnace, Tianjin City, China). The temperature program was as follows: initial heating to 100°C for about 1 h, and to 620°C for about 3 h, followed by natural cooling of the furnace to room temperature. The channels were typically 20  $\mu\text{m}$  deep and 50–60  $\mu\text{m}$  wide at half-depth. The separation length was 3.0–3.5 cm. For forming reservoirs connected to the microchannels, the 2 mm diameter holes in the top glass plate (either substrate or cover plate) were drilled by the CK-250L ultrasound driller (Shantou Goldstar Ultrasonic Machinery, China). The typical volume of the reservoirs was 15  $\mu\text{L}$ .

## 2.5 Microchip electrophoresis

The electroosmotic flow in the channels was minimized using PVP-TBE buffer as a dynamic coating [17]. The channels were filled with a sieving buffer solution for microchip gel electrophoresis after they were oxidized in boiling  $\text{H}_2\text{SO}_4/\text{H}_2\text{O}_2$  (1:1) for 10–15 min, followed by washing with deionized  $\text{H}_2\text{O}$ . The coating was stable for multiple injection/separation cycles and provided reproducible separation performance. For DNA fragment sizing, 2.5% PVP solution in a 100 mM Tris/100 mM boric acid/2 mM EDTA buffer was used. An intercalating dye, SYTOX Orange nucleic acid stain, was added to the polymer solution at 1  $\mu\text{M}$  for the PCR on-chip experiments. A DNA marker containing 11 DNA fragments of 100, 200, 300, 400, 500, 600, 700, 800, 900, 1000, and 1500 bp at approximately equal weight/volume concentration was used for PCR verification, product size determination, and estimations of the amplification efficiency. For the laser-induced fluorescence (LIF) detection, the LIF microfluidic chip analyzer was used. For the conventional injection/separation cycle, the sample was first loaded into the sample reservoir and then injected by applying 400 V/cm at the sample waste and grounding the sample reservoir for 30 s. The buffer and waste reservoirs had no potentials applied since the low diffusion coefficients of DNA fragments in the polymer sieving medium resulted in no substantial increase in the injection plug length or deterioration of separation channel. The relative potentials were switched to 0, 1.1, 0.3, and 0.3 kV at the buffer, waste, sample, and sample waste reservoirs, respectively.

## 2.6 Thermal cycling on-chip

Figure 2a shows a picture of the thermal cycler for the micro-PCR device, which was designed and built in-house using two Peltier thermoelectric devices (1 inch  $\times$

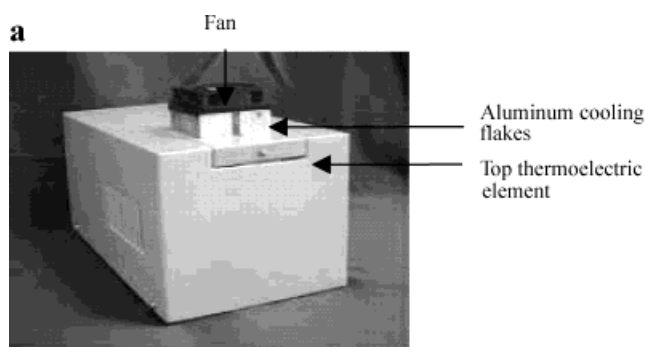
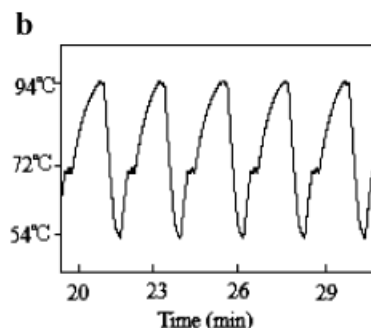


**Figure 2.** (a) Thermal cycler for the micro-PCR device (home-made); (b) temperature cycling trace curve of the PCR chip.

1 inch, output power of 30 W). Aluminum cooling flakes are attached to the backside of the Peltier devices as heat sinks. A small cooling fan was also attached to each of the two aluminum blocks for convective cooling. During PCR thermal cycling, the 2/3 area of the entire chip was sandwiched between the two Peltier elements. The device temperature and Peltier surface temperature were monitored using thermocouples. Software in-house made was used for thermal cycle temperature control. A drop of mineral oil on the bottom Peltier element ensured good thermal contact with the cycled region of the chip. All microchannels and reservoirs, excluding the PCR reaction area (including sample reservoir) in Fig. 1, were filled with sieving solution. The reaction well was first treated with 2.5 g/L bovine serum albumin (BSA) solution for 2–3 min to modify the inner glass surface of the milled reservoir. The BSA was then removed from the well and replaced with 3.5–4  $\mu\text{L}$  of the PCR reaction mixture (individual or duplex PCR reaction mixture and cDNA of the sample). To prevent evaporation, all wells were topped with 6–7  $\mu\text{L}$  of mineral oil. The temperature steps were 94°C for 2 min, followed by 94, 55, and 72°C with holding times of 45, 30, and 30 s for 30 cycles, and then 72°C for 2 min to perform DNA amplification. The top thermoelectric element of the thermal cycler for the micro-PCR device was not placed in direct contact with the chip in order to eliminate the requirement of sealing the top reaction reservoir against contact-driven capillary wicking. Thus, the top assembly was positioned over the chip using 0.5 mm thick graphite strips as spacers.

## 2.7 Detection system

Figure 3 shows schematically the layout of a micro-CE device with integrated confocal laser fluorescence detector and automicromanipulation stage. The dimensions





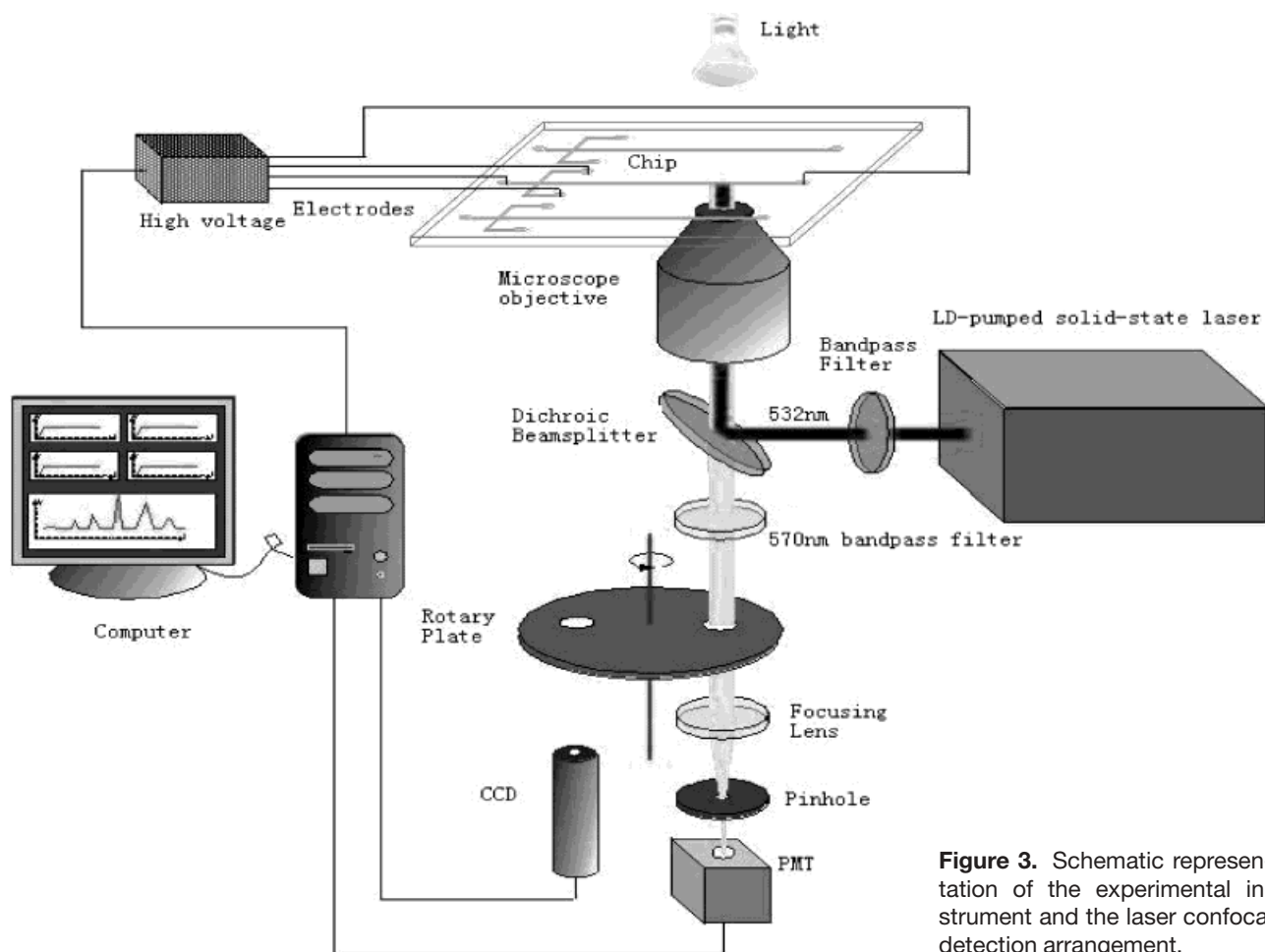


**Figure 3.** Schematic representation of the experimental instrument and the laser confocal detection arrangement.

of the instrument were  $50 \times 50 \times 45$  cm. The output radiation (532 nm) from an air-cooled laser diode (LD)-pumped solid-state laser (20 mW; Mektec Seiwa Corporation, Beijing, China) passes through a 532 nm filter (Omega Optical, Brattleboro, VT, USA). The beam is reflected by a dichroic beam-splitter (Omega Optical) and focused into the channel through a  $20\times$  microscope objective (0.4 N.A.). The emission signal is collected by the same objective and transmitted back through the dichroic beam-splitter. The emission beam passes through a bandpass filter (Omega Optical), which may be alternated easily to fit a wide selection of dyes, and is focused by a focusing lens through a  $400 \mu\text{m}$  pinhole. The photomultiplier tube (R212; Japan) is mounted in an integrated detection module including high-voltage power supply, voltage divider, and amplifier. The charge-coupled device (CCD) camera was fixed at the same board as the photomultiplier tube in order to focus and observe the channel. The whole optical system was installed on the X-Y-Z translational stage (3-D micro-

manipulator, adjusting precision  $1 \mu\text{m}$ ), and the focus can be controlled *via* the picture displayed on the screen.

### 3 Results and discussion

#### 3.1 Detection limit of the detection system

The detection limit of Rhodamine 6G dye for the detection system with the home-made chip and a 100 mM TBE buffer is  $6.67 \times 10^{-13} \text{mol/L}$  ( $S/N > 3$ ). The linear range of detection was  $4.02 \times 10^{-6} \text{mol/L}$  to  $4.02 \times 10^{-9} \text{mol/L}$  ( $r = 0.9996$ ). For detailed information we refer to the literature [18]. A  $50 \text{ ng}/\mu\text{L}$   $\Phi$  X-174/*Hae*III digest DNA marker, with restriction fragments ranging in size from 72 to 1353 bp (72, 118, 194, 234, 271, 281, 310, 603, 872, 1078, 1353 bp), was serially diluted and determined on the detection system. When the S/N of the 603 bp fragment was  $\geq 3$ , its corresponding concentration was

0.2 ng/ $\mu$ L (the mass of the 603 bp fragment detected was 3.36 fg according to the injection volume). These data show that this detection system has a high sensitivity, which is over 100-fold higher than that of agarose gel electrophoresis in the conventional PCR assay [18]. The high assay sensitivity is important for early diagnosis of the diseases and early identifying of the suspected patients with SARS.

### 3.2 Design and optimization of SARS-CoV RT-PCR assay kit

Primers were designed according to the conserved regions of open reading frame 1b (replicase 1B) following the Tor 2 SARS genome sequence in order to amplify sequences within two regions of SARS genome, 15240–15612 and 17743–18349. Multiplex PCR is a modification of the basic PCR method, where multiple pairs of primers are used in the same reaction [19, 20]. A multiplex protocol appears to be useful for the investigation of different target sequences at the same time. By RT to cDNA and subsequent amplification, the RNA template can also be amplified by multiplex PCR. The SARS RNA genome is apt to mutation, which may lead to primers ill-matched with templates. Multiplex PCR, which can effectively reduce the possibility of false-negative PCR results caused by genome instability, amplifies different regions at the same time. So we designed nine pairs of primers according to the Tor 2 SARS genome sequence, and 2 of 9 pairs of primers were optimized as the primers for RT-PCR SARS-CoV assay kit. The sequences of two pairs of the primers are 5'-TAGGATTGCCTACGCAGACT-3' and 5'-AGAGCCATGCCTAACATGCT-3' (for the 240 bp product), and 5'-ATTGGCTGTAACAGCTTGAC-3' and 5'-TAGGGTAACCATTGACTTGG-3' (for the 438 bp product), respectively. The concentration of  $Mg^{2+}$ , enzymes, reaction time, cycling times, etc., for RT-PCR SARS-CoV assay kit were optimized. Optimization of RT-PCR SARS-CoV assay with SARS-CoV from the cultured Vero-E6 cells was finished by the GeneAmp PCR system 2400 (Perkin-Elmer) thermocycler. Reaction products from duplex PCR were analyzed by agarose gel electrophoresis (Fig. 4).

### 3.3 PCR-CE on-line

A series of thermal transfer experiments have been conducted using different thicknesses of the glass (e.g., 2 mm, 0.5 mm, 0.15 mm), and it was found that the intra-reservoir temperature would fit the set point temperature better by using a thinner glass cover (data not shown). However, the thinnest glass cover plate of the bottom of every reservoir is easily shattered, particularly during installation of the electrodes. Therefore, the thickness of the

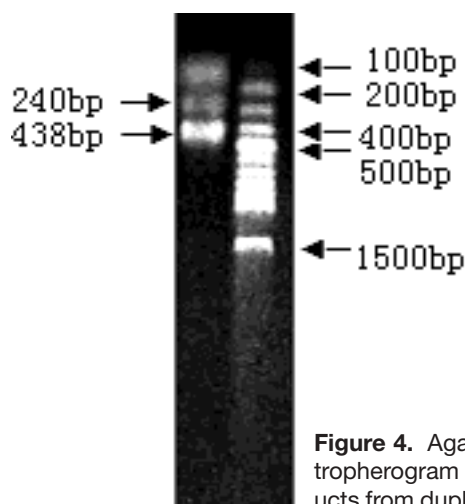


**Figure 4.** Agarose gel electropherogram of the products from duplex PCR.

glass cover plate was kept thin (0.5 mm) in order to achieve a reasonable thermal cycle time. The temperature cycling of the PCR chip in a dual Peltier assembly is represented by trace curve in Fig. 2b, which shows the temperature profile for five cycles of the program in-house software. The Peltier surface temperature and intra-reservoir temperature were measured by thermocouples. A built calibration chip contained an embedded thermocouple to assess the intra-reservoir temperature and compare it with the temperature of the Peltier surface. These data were used to design the thermal cycle profile of amplification experiments. The chips used in the experiments did not have the embedded thermocouple. Cycle times were initiated according to the intra-reservoir temperature.

Successful DNA amplification is dependent on the preliminary treatment of PCR reservoirs as well as on the reaction mixture volume. The pretreatment of PCR reservoirs was performed as described by Khandurina *et al.* [15]. Optimum thermal uniformity during heating/cooling cycles resulting in a good PCR efficiency was achieved using 3–4  $\mu$ L PCR cocktail in 2 mm diameter reaction reservoirs and a serpent-shape channel. To achieve PCR amplification, a pair of PCR primers was first performed on the chip thermal cycler, and then the duplex PCR was manipulated. Figure 5a shows the electropherogram of 240 and 438 bp PCR products of the positive control of SARS-CoV. Amplification and electrophoretic analysis were on the same chip. The total analysis time was approximately 50–60 min including 30 thermal cycles and electrokinetic injection/separation manipulation. Figure 5b shows the electropherogram of the negative control (parainfluenza virus) and Fig. 5c the electropherogram of the 240 and 438 bp PCR products of the cultured SARS-CoV. To identify the length of unknown amplified products or verify the sizes of known target sequences, PCR prod-

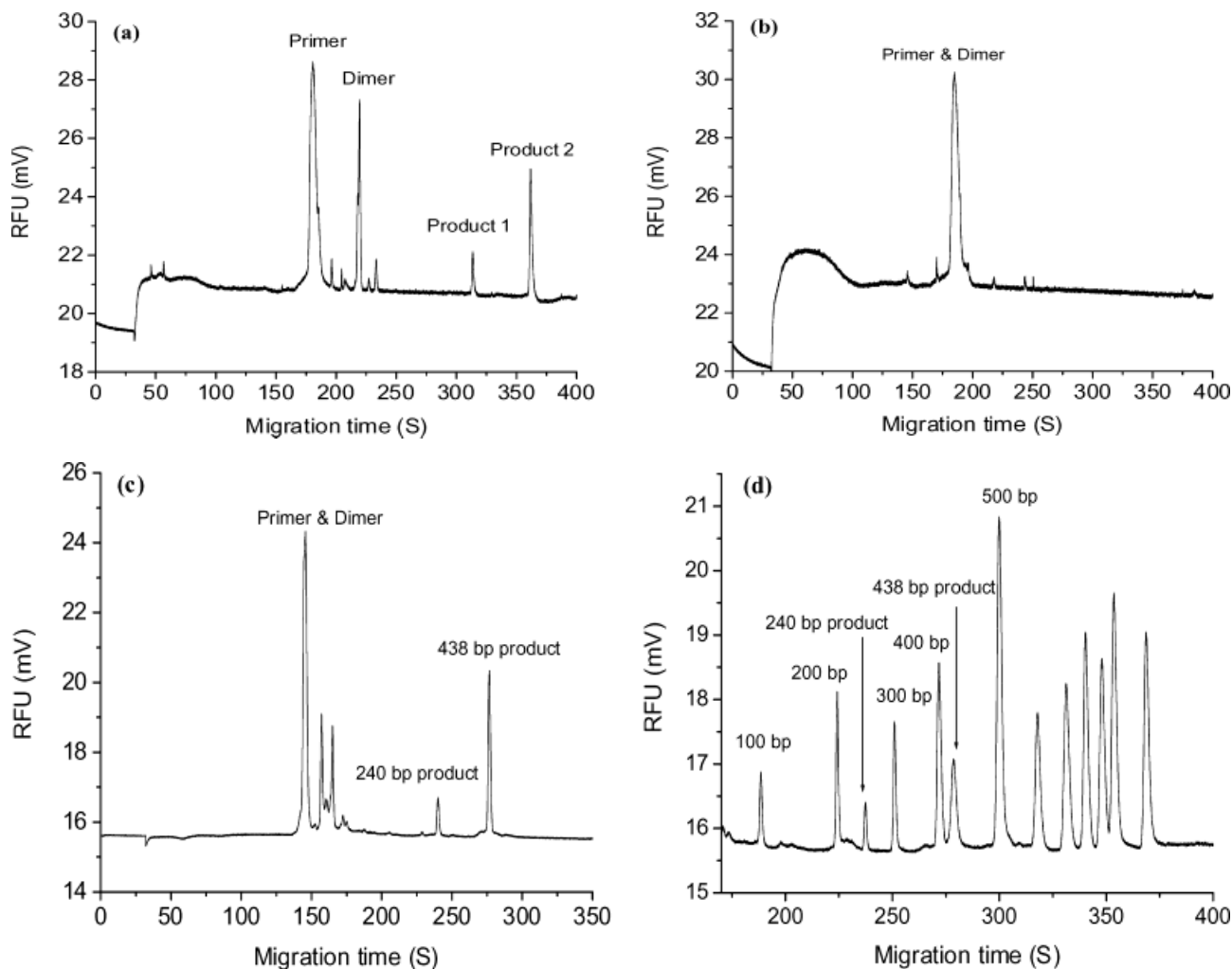


**Figure 5.** Microfluidic chip electropherograms. (a) Positive control; (b) negative control; (c) cultured SARS-CoV (240 and 438 bp PCR products); (d) PCR product + 100 bp DNA marker.

ucts were mixed and coelectrophoresed with size markers of DNA as demonstrated in Fig. 5d for 240 and 438 bp products. The latter profile was obtained by simply adding a DNA marker solution to the sample reservoir containing the PCR product after mixing. Compared to the standard curve of the migration time vs. the fragment size of DNA marker, the size of the amplified DNA fragments was determined by their migration time.

### 3.4 Determination of the clinical specimens

All RNA of SARS-CoVs was extracted from 18 clinical SARS samples with RNAeasy Mini Kit (Qiagen) before performing the RT-PCR reaction. The RT reactions with the extracted RNA were performed on a conventional PCR cyler to get the cDNA of the sample. After chip-

PCR with cDNA of the sample, the PCR chip was translated on the detection system to separate the PCR products. The chip-PCR and on-line CE separation for each sample were therefore performed on the chip (Fig. 1). Seventeen positives were achieved from 18 of the nasopharyngeal swabs from the clinically diagnosed patients with SARS by the microfluidic chip system. However, Fig. 6 shows that 12 positives of 18 SARS samples noted above were detected by the conventional PCR with agarose gel electrophoresis.

## 4 Concluding remarks

A microfluidic chip system was developed and successfully used in determining the SARS-CoV of specimens from clinically diagnosed SARS patients. The positive

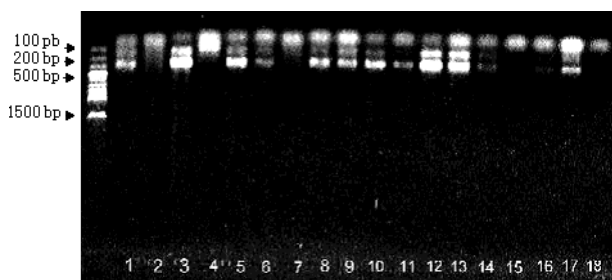


**Figure 6.** Gel electropherogram of the positive products of RT-duplex PCR for the nasopharyngeal swabs of 18 clinically diagnosed patients with SARS.

rate of the SARS-CoV for clinical SARS samples is up to 94.44% (17/18) using this system. The positive rate achieved by the conventional RT-PCR with agarose gel electrophoresis system was only 66.67% (12/18). Compared to the conventional system, the microfluidic chip system showed a higher positive rate (>27%), shorter testing time, and the potential application of determining the SARS-CoV of specimens.

*The authors thank the First Military Medical University for providing samples of clinically diagnosed SARS patients. This research was sponsored by the National Science Council of the People's Republic of China under contract Nos. 20275039, 20035010, and 20299030, and in part by the Chinese Academy of Sciences for building the microfluidic chip analyzer and by the Dalian Institute of Chemical Physics, Chinese Academy of Sciences for studying SARS.*

Received December 30, 2003

## 5 References

- [1] WHO Summary table of SARS cases by country, 1 November 2002–7 August 2003, [www.who.int/csr/sars/country/2003\\_08\\_15/en/](http://www.who.int/csr/sars/country/2003_08_15/en/).
- [2] SARS: Laboratory diagnosis tests. 29 April 2003, <http://www.who.int/csr/sars/diagnostictests/en>.
- [3] McIntosh, K., *Clin. Chem.* 2003, **49**, 845–846.
- [4] Hoard, J. C., Schultz, T. F., in: Collins, M., Clifton, N. J. (Eds.), *Methods in Molecular Biology*, Humana Press, Totowa, NJ 1991, Vol. 8.
- [5] Poon, L. L. M., Wong, O. K., Luk, W., Yuen, K. Y., Peiris, J. S. M., Guan, Y., *Clin. Chem.* 2003, **49**, 845–846.
- [6] Wu, X. W., Cheng, G., Di, B., Yin, A. H., He, Y. S., Wang, M., Zhou, X. Y., He, L. J., Luo, K., Du, L., *Chin. Med. J.* 2003, **116**, 988–990.
- [7] Freemantle, M., *Chem. Eng. News* 1999, **22**, 27–36.
- [8] Northrup, M. A., Benett, B., Hadley, D., Long, G., Landre, P., Lehew, S., Richards, J., Stratton, P., *Anal. Chem.* 1998, **70**, 918–922.
- [9] Belgrader, P., Benett, W., Hadley, D., Long, G., Mariella, R., Milanovich, F., Nelson, W., Richards, J., Stratton, P., *Clin. Chem.* 1998, **44**, 2191–2194.
- [10] Belgrader, P., Benett, W., Hadley, D., Richards, J., Stratton, P., Mariella, R., Milanovich, F., *Science* 1999, **284**, 449–450.
- [11] Ibrahim, M., Lofts, R., Jahrling, P., Henchal, E., Weedn, V., Northrup, M. A., Belgrader, P., *Anal. Chem.* 1998, **70**, 2013–2017.
- [12] Belgrader, P., Smith, J., Weedn, V., Northrup, M. A. J., *Forensic Sci.* 1998, **43**, 315–319.
- [13] Effenhauser, C. S., Bruin, G. J. M., Paulus, A., Ehrat, M., *Anal. Chem.* 1997, **69**, 3451–3457.
- [14] Yang, J., Liu, Y. J., Rauch, C. B., Stevens, R. H., Liu, R. L., Lenigk, R., Grodzinski, P., *Lab Chip.* 2002, **2**, 179–187.
- [15] Khandurina, J., Mcknight, T. E., Jacobson, S. C., Waters, L. C., Foote, R. S., Ramsey, J. M., *Anal. Chem.* 2000, **72**, 2995–3000.
- [16] Woolley, A. T., Mathies, R. A., *Proc. Natl. Acad. Sci. USA* 1994, **91**, 11348.
- [17] Kopp, M. U., deMello, A. J., Manz, A., *Science* 1998, **280**, 1046–1047.
- [18] Zhou, X. M., Dai, Z. P., Luo, Y., Liu, X., Wang, H., Lin, B. C., *Chem. J. Chin. Univ.* 2004, **3**, 336–340.
- [19] Valassina, M., Cuppone, A. M., Cusi, M. G., Valensin, P. E., *Clin. Diagn. Virol.* 1997, **8**, 227–232.
- [20] Cassinotti, P., Mietz, H., Siegl, G., *J. Med. Virol.* 1996, **50**, 75–81.